



## Multi-stimuli Responsive Natural Fibers Immobilized with Silver Nanoparticles via Plasma-activated Generation of Polyaniline



Tawfik A. Khattab<sup>a,\*</sup>, Hamada M. Mashaly<sup>a</sup>, Hend Ahmed<sup>a</sup>, Mohamed Rehan<sup>b</sup>, Azza A. El-Halwagy<sup>a</sup>

<sup>a</sup> Dyeing, Printing and Auxiliaries Department, Textile Industries Research Division, National Research Centre, 33 El-Buhouth Street, Dokki, Cairo 12622, Egypt.

<sup>b</sup> Pretreatment and Finishing of Cellulosic-based Fibers Department, Textile Industries Research Division, National Research Centre, 33 El-Buhouth Street, Dokki, Cairo 12622, Egypt.

### Abstract

Functionalization of natural fibers with electroactive polymeric materials can create conductive surfaces with multifunctional properties. Herein, we develop smart fibers using plasma supported coating of wool fabrics with various polyaniline derivatives (PANi) in the presence/absence of *in-situ* prepared silver nanoparticles (AgNPs). Nanostructural thin film of PANi was synthesized *in-situ* employing plasma-pretreatment to assess the polymerization process. AgNPs were immobilized *in-situ* during the formation of PANi starting from silver nitrate (AgNO<sub>3</sub>) by taking benefit of the reducing ability from the electroconductive polymer derivatives. Some selected electroactive polymers were applied starting from aromatic amines, including *m*-anisidine, *o*-phenylenediamine and *p*-nitroaniline. The morphological characteristics of the produced fabrics were studied by scan electron microscope (SEM). The chemical analysis was studied by energy-dispersive X-ray analyzer and Fourier transform infrared (FTIR) spectra. As monitored by CIE Lab colorimetric measurements, instant reversible color variations were monitored by recording the colorimetric measurements of the produced sensor fabrics. By changing the sort of the electroactive polymer and the inclusion of silver nanoparticles, the imparted characteristics of the developed wool fabrics, including antimicrobial, electroactivity and stimuli-responsive effects were explored for a diversity of promising medical applications.

**Keywords:** Plasma; Wool; Chromism; Antimicrobial; Electrical conductivity.

### 1. Introduction

Smart textiles are responsive fabrics or fibers with the ability to monitor and interacting with different stimuli, such as heat, electricity, and acid/base conditions as well as detection of pathogenic microorganisms and hazardous chemicals [1-3]. The sensing performance of smart textiles occurs either manually or in a preprogramming manner in response to such external stimuli in various modes, such as lighting up in particular patterns, visual color shift and/or even acting as an electronic display presenting pictures and video [4, 5]. The response of smart chromic textiles depends mainly on color change, such as thermochromic, halochromic and photochromic textile products which can change their color in response to heat, pH and light, respectively [7-12]. The conventional functions of textile products were to protect human from cold and rain. Currently, a novel generation of textile products known as smart or interactive clothing has been raised. Smart fabrics are a relatively novel discipline in the textile industry. They are reactive substrates able to function as sensors or actuators. Their potential functions are enormous as they can act as, for example, monitors and protective materials for human healthcare from any environmental hazardous

conditions by warning from an approaching danger [13-17]. Thus, there has been a considerable interest on the exploration of chromic organic substances, such as sensing colorants and electroconductive polymers [18, 19]. The electrical properties of polymers can be attributed to their conjugated polymer chains. Electroconductive polymers are promising materials for developing tools for multifunctional applications, such as supercapacitors, flexible and transparent displays, organic light emitting diodes, batteries, organic photovoltaics, electronic circuits, electrochromic smart windows, electroluminescent devices, actuators, and electrochemical and chemical sensors and biosensors [20-26]. Furthermore, electroconductive polymers have been employed for electromagnetic interference shielding substrates, particularly as a radar absorber coating on stealth aircrafts. There have been a variety of materials that have been explored as radar absorption substrates, such as metal oxide nanoparticles, electrically conductive polymers and high performance textiles [27-29]. The blocking efficiency of electromagnetic interferences depends essentially on the characteristics of the functionalized filler, including its thickness, distribution and dielectric constant. Silver nanoparticles employed as a

\*Corresponding author e-mail: [ta.khattab@nrc.sci.eg](mailto:ta.khattab@nrc.sci.eg); (Prof. Tawfik A. Khattab).

EJCHEM use only: Receive Date: 29 June 2021, Revise Date: 24 July 2021, Accept Date: 15 August 2021

DOI: [10.21608/ejchem.2021.83132.4081](https://doi.org/10.21608/ejchem.2021.83132.4081)

©2022 National Information and Documentation Center (NIDOC)

filling agent in polymeric matrices which can be coated on insulator substrates to give nanocomposite coatings with enhanced microwave absorption. AgNPs are distinguished with their efficient electrical conductivity and antimicrobial activity [30-33].

There has been a diversity of *para*-conjugated polymers, such as polythiophenes, polypyrroles and polyanilines. Among these *para*-conjugated polymers, polyaniline (PANI) derivatives have been broadly applied owing to their simple preparation process, low cost, unique electrochemical properties, and chemical and thermal stability. Thus, polyaniline derivatives have been the earlier commercially available conjugated polymers [34-36]. Nonetheless, the industrial application of polyanilines has a number of disadvantages, such as weak processing and poor mechanical properties. Improving their mechanical performance could be accomplished by producing nanocomposites of polyanilines with conventional nonconductive polymers or textile substrates [37, 38]. There are various polymerization techniques to prepare polyaniline-coated fibers, such as graft and block polymerization as well as chemical, plasma and electrochemical approaches [39-43]. The plasma technology has been applied on fabrics/fibers surfaces as an eco-friendly approach to modify only the upper atomic surface layers of a fabric without influencing the matrix properties of the fabric. Despite the plasma excited species are mainly highly energetic electrons which are randomly to some extent breaks down chemical bonding; the plasma activated substrates can be preserved under ambient conditions [44, 45].

Herein, we report on the development of an active and passive hybrid wool fabric due to their multifunctional performance including thermochromic, electroconductive and antimicrobial properties. Wool fabric was pretreated with plasma to provide *in-situ* polymerization process of aromatic polyamines, including poly (*o*-phenylenediamine), poly (*p*-nitroaniline) and poly (*m*-anisidine) to provide consistent nano-sized structural thin layers in the presence/absence of silver nitrate which is able to go through an oxidation/reduction process affording silver nanoparticles/aromatic polyamine immobilized onto plasma activated wool fibers. Wool is a naturally occurring fiber characterized with its ability to resist wrinkles, hypoallergenic, naturally anti-static and flame resistant, balanced thermal insulation properties, easy to clean. It is eco-friendly and sustainable due to its biodegradation ability. The generation of PANi or AgNPs/PANi film on wool surface and its sensory effects were explored by EDX, FTIR, SEM and coloration measurements. Both of antimicrobial and electroactivity of the treated wool fabrics were explored. The multifunctional characteristics of the treated wool fabrics, including antibacterial, electroactivity and thermochromic performance were investigated.

## 2. Experimental

### 2.1. Materials and reagents

Wool fabric (100 %) was obtained from Misr-Helwan Company for Spin and Weave, Egypt. The wool substrate was subjected to scouring in an aqueous medium (1:50) enclosing non-ionic detergent (2 g L<sup>-1</sup>; Hostapal, Clariant, Swiss) and Na<sub>2</sub>CO<sub>3</sub> (2 g.L<sup>-1</sup>). The scouring process was carried out at 50°C for thirty minutes to remove wax-based

substances and other impurities. This was followed by washing using tap water, and finally air-drying. Silver nitrate (AgNO<sub>3</sub>), *o*-phenylenediamine, *m*-anisidine and *p*-nitroaniline were obtained from Sigma Aldrich.

### 2.2. Incorporation of AgNPs/PANi onto wool fibers

As displayed in **Figure 1**, the wool substrate (5x5 cm) was fixed among two electrodes and subjected to treatment with plasma for 7 minutes under ambient conditions using a current of 5 mA, followed by pad-dry-cure (Pickup of 90%) using an aqueous mixture (liquor ratio of 1:50) of aromatic amine (10.0 mmol) and CH<sub>3</sub>CO<sub>2</sub>NH<sub>4</sub> (20.0 g L<sup>-1</sup>) at 30°C for thirty minutes. The wool sample was subjected to washing with water, and finally subjected to air-drying. In the case of *in-situ* preparation of AgNPs, plasma-pretreated wool sample was exposed to padding (Pickup of 90%) in an aqueous mixture (liquor ratio of 1:50) of silver nitrate (100 ppm), arylamine (10.0 mmol) and CH<sub>3</sub>CO<sub>2</sub>NH<sub>4</sub> (20.0 g.L<sup>-1</sup>).

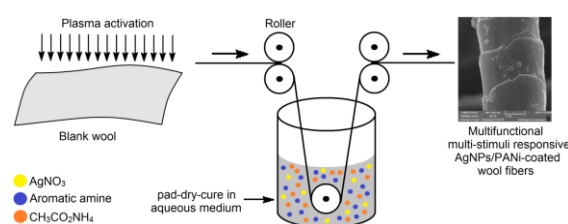


**Figure 1.** Diagram representing the *in-situ* production of smart fibers.

### 2.3. Sensor testing

The vapochromic testing was investigated by exposing the wool substrates to vapors of HCl, while the acidochromic capability to acidic aqueous media was studied by soaking wool in an aqueous HCl (0.1 N) [3]. The treated wool samples were soaked in aqueous solutions of Fe<sup>+3</sup> or Cu<sup>2+</sup> (0.1 N) to explore their metallochromic performance. The thermochromic activity was examined at ~65°C via exposure of the wool substrates to hot-air released from a heating gun (ORS-NascoMaster, 467HG301A). The immediate color variation of the tested wool substrates was studied and proved visually and by measuring their coloration measurements [2]. The pH value was monitored using BECKMAN-COULTER meter (pHI340).

### 2.4. Characterization and measurements

#### 2.4.1. Plasma setup management

The experimental system composed of two copper-based flat and parallel electrodes with a 2.5 cm diameter and at a 1.1 mm distance from each other. Electrodes were coated with porous Al<sub>2</sub>O<sub>3</sub> sheet with a diameter of 4.0 cm and a thickness of 3.5 mm. Voltage converter (1-10 kV) was applied as an electricity generator providing sinusoidal voltage at a 50 Hz. The discharge system functioned as an air opening. Both passing current (I) and electric plates functional potential (Va) were recorded using HAMEG/HM407 oscilloscope at 40 MHz. The current was determined using the reducing voltage crossing the resistant unit (R<sub>1</sub>=100) attached to discharging unit to ground. The voltage crossing plates was measured using the resistance separator (R<sub>2</sub>/R<sub>3</sub>= 500).

#### 2.4.2. Fourier-transform infrared spectrophotometer

FT-IR spectral profiles (400-4000  $\text{cm}^{-1}$ ) were reported [17] using Nexus-670 (Nicolet, USA).

#### 2.4.3. Scan electron microscopy

SEM micrographs were reported by two different instruments, including Quanta/FEG/250 (Czech Republic) and VEGA 3, TESCAN.

#### 2.4.4 Energy-dispersive X-ray analyzer

SEM equipment is connected to TEAM/EDX energy dispersive X-ray analytical tool for determining the chemical composition applying an accelerating voltage at 20 kV. The average diameters of nanoparticles were monitored using Image J program.

#### 2.4.5. Electroactivity assessment

The electrical conductivity of both untreated and treated wool samples was measured [19] by HIOKI LCR Hi 3522-50 testing apparatus (Japan).

#### 2.4.6. Antimicrobial activity

The antimicrobial performance of the cured wool fibers was tested quantitatively against some bacterial pathogens, including *S. aureus* and *E. coli* applying AATCC 100-1999 as a standard procedure [17].

#### 2.4.7. Coloration and colorfastness screening

Ultra Scan PRO spectrophotometer with  $10^\circ$  standard viewer and D65 illuminant (Hunter Lab, USA) was employed to investigate the color change of the tested sensor wool fabrics applying tinctorial strength ( $K/S$ ) and CIE Lab.  $L^*$  is denoted as blackness (0) to whiteness (100),  $a^*$  is denoted as greenness (-) to redness (+), and  $b^*$  is denoted as blueness (-) to yellowness (+) color ratios. The colorfastness properties were recorded according to ISO105(X12:1987) for rubbing, ISO105-C02(1989) for washing, ISO105(E04:1989) for perspiration, and ISO105(B02:1988) for light [46, 47].

### 3. Results and discussion

#### 3.1. Fabrication of functional wool fibers

Wool was treated with plasma under ambient conditions, followed by treatment with aromatic amine to afford an electroactive polymer layer on the wool fiber surface via *in situ* polymerization. In the same way, the wool fibers were subjected to the same treatment procedures in presence of  $\text{AgNO}_3$  to give a composite film of silver nanoparticles, aromatic polyamine and wool fibers (AgNPs/PANi/wool). The inspiration of this research aimed to create electroactive and antimicrobial wool fibers imparted with multi-stimuli responsive sensory effects. The incorporation of AgNPs was performed *in-situ* onto the surface of wool fibers during the polymerization course of the polyaniline derivative from the reduction of  $\text{AgNO}_3$ . This led to a reduced production price of silver nanoparticles/PANi/wool fibers owing to the reduced extra cost from the synthesis and incorporation procedures of AgNPs onto the fibers. Silver nitrate ( $\text{Ag}^+$ ) was exposed to an *in-situ* reduction to  $\text{Ag}^0$  during polymerization of aniline derivatives to give the corresponding polyaniline reactive polymer which turns out in the oxidized molecular structure form concurrently. The total contents of  $\text{Ag}^0$  were confirmed on poly (*p*-nitroaniline) incorporated onto wool substrate using EDX spectroscopy. The polymerization mechanism of the aniline

derivatives to afford the corresponding polyaniline and AgNPs is displayed in **Figure 2**.

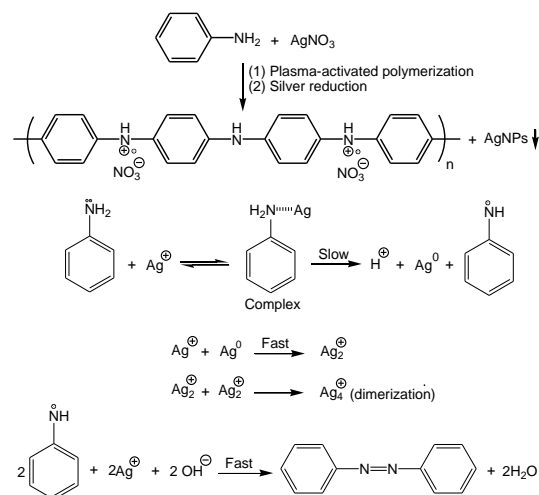


**Figure 2.** Plasma-assisted *in-situ* polymerization of aniline derivatives using  $\text{AgNO}_3$  as an oxidizing agent.

#### 3.2. Morphological characteristics

The structure morphology of both PANi/wool and AgNPs/PANi/wool fabrics were studied by SEM, FTIR and EDX spectroscopy. Pristine wool fibers (**Figure 3a**) showed a smooth surface, while the blank plasma-activated wool (**Figure 3b**) displayed a surface with etches and grooves. Compared to pristine wool fibers, the nano-sized structures of either PANi or AgNPs/PANi films were homogeneously deposited onto the treated fabrics via *in situ* polymerization and redox conditions. However, the produced Ag NPs/PANi layer (**Figure 3c**) was more consistently distributed on the fiber surface compared to PANi layer (**Figure 3d**), which demonstrated a slight affinity to generate cluster-based architectures. This can be assigned to the enhanced binding of Ag NPs/PANi hybrid to plasma-pretreated wool by Ag-Oxygen bonding. Moreover, the structural morphology of Ag NPs/PANi was in the nano- and microparticle size that are preferred to enhance the electroconductivity [44]. The three conjugate polyaniline derivatives, including poly(*o*-phenylenediamine), poly(*m*-anisidine) and poly(*p*-nitroaniline) were capable to reduce ionic  $\text{Ag}^+$  in  $\text{AgNO}_3$  into metallic  $\text{Ag}^0$  that was produced as AgNPs incorporated as a composite within the oxidation form of PANi derivative. No significant distinctions were observed in the morphologies of the three polyaniline derivatives. The size distribution of the produced nano/micro-sized structures of AgNPs/PANi incorporated onto wool fibers was measured using software program connected to scanning electron microscope. For the three electrically active polyaniline derivatives, the diameter distribution of either PANi or AgNPs/PANi on the wool fibrous surface was not homogeneous in size. The particle size of both PANi and AgNPs/PANi was ranging between 280 nm and 5.5  $\mu\text{m}$ , and 220 nm to 2.0  $\mu\text{m}$ , respectively.

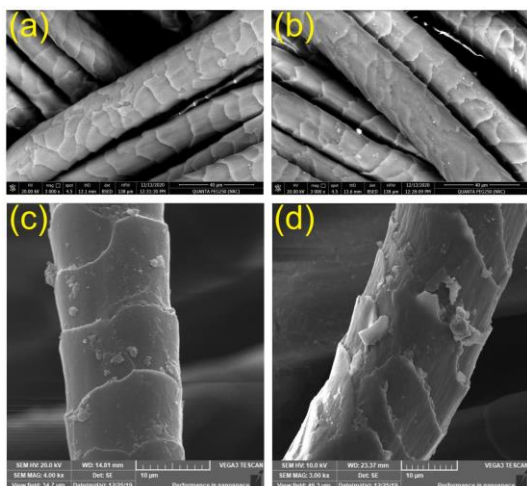


**Figure 3.** SEM images of pristine wool (a), blank plasma-activated wool (b), as well as AgNPs/poly(*p*-nitroaniline) (c), and poly(*p*-nitroaniline) (d) incorporated onto plasma-activated wool fibers.

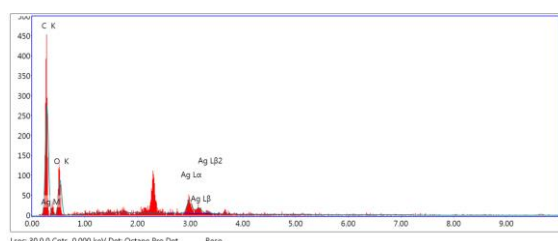


**Figure 4.** EDX diagram of AgNPs/poly(*p*-nitroaniline) incorporated onto plasma-activated wool fibers.

The major elemental composition of AgNPs/PANi incorporated onto plasma-activated wool substrates was studied using EDX spectroscopy by reporting the chemical content at two selected surface locations of the tested wool substrate as monitored in **Figure 4** and **Table 1**. The total content of the detected elements were almost the same at these two surface locations confirming the homogeneous dispersion of Ag NPs/PANi onto the tested surface of wool fabric.

**Table 1.** Major elemental composition (Wt%) of blank and AgNPs/PANi(*p*-nitroaniline) on plasma-activated fabrics.

Wool fabrics		C	O	Ag
Pristine		63.86	36.14	0
AgNPs/PANi (plasma-activated)	Spot 1	57.01	36.8	6.19
	Spot 2	57.54	36.59	5.87

FTIR spectral profiles were utilized to explore the main absorbance bands of Ag NPs/PANi integrated onto plasma-pretreated wool fibers, including both hydroxyl (OH) and CH aliphatic groups. FTIR spectra of pristine wool, PANi/wool and AgNPs/PANi/wool fabrics are shown **Figure 5**. Generally, there are no substantial changes were observed in the absorption bands. The characteristic peaks of blank wool were detected at 3287  $\text{cm}^{-1}$  (stretching

hydroxyl) and 2932  $\text{cm}^{-1}$  (stretch aliphatic CH). An absorption amide I peak was observed at 1633  $\text{cm}^{-1}$  is associated with the stretching vibrations of the carbonyl group; while the absorption amide II peak at 1524  $\text{cm}^{-1}$  was attributed to the bending deformation of NH bonding and stretching vibrations of C–N bonds. The amide III at 1247  $\text{cm}^{-1}$  belongs to C–N stretching bonding and NH in-plane bend vibrations. Compared to FTIR spectrum of pristine wool, PANi/wool and AgNPs/PANi/wool fibers didn't show new peaks proving that no considerable chemical interactions took place to the fiber surface throughout the inclusion of either polyaniline or AgNPs/polyaniline onto the wool fibers, respectively.

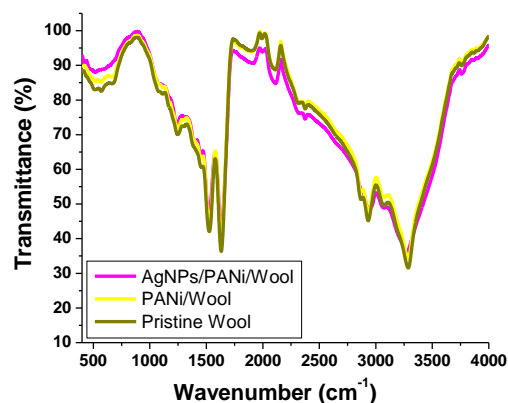


**Figure 5.** FTIR spectra of pristine, PANi(*p*-nitroaniline) and AgNPs/PANi(*p*-nitroaniline) on wool fibers.

### 3.3. Electroactivity performance

The surface electroactivity of PANi/wool and AgNPs/PANi/wool with/without plasma-pretreatment was studied using *p*-nitroaniline as a model (**Table 2**). The electroconductivity of blank wool was  $1.2 \times 10^{-8}$  S/cm, whereas the conductivity of the coated wool fabrics was ranging between  $2.2 \times 10^{-5}$  and 0.6457 S/cm. The electroactivity of PANi incorporated onto wool was less than that of AgNPs/PANi incorporated onto wool fibers. Plasma-pretreated wool fibers demonstrated improved electroconductivity compared to the plasma-pretreated fibers. This might be attributed to AgNPs facilitating the conduction path in PANi composite. Silver nanoparticles acted as a suitable pattern for the formation of well-oriented PANi to result in an enhanced electron charge transfer. In general, the electrical conductivity was enhanced upon adding AgNPs to the PANi matrix, which can be assigned to the synergistic character of AgNPs [48].

**Table 2.** Electroconductivity and antimicrobial properties of blank and PANi(*p*-nitroaniline) and AgNPs/PANi(*p*-nitroaniline) loaded onto wool fibers with/without plasma-pretreatment.

Wool sample		Conductivity (S cm <sup>-1</sup> )	Antimicrobial Reduction Percentage	
			<i>E. coli</i>	<i>S. aureus</i>
blank		1.2 × 10 <sup>-8</sup>	0.00	0.00
PANi	Without plasma	2.2 × 10 <sup>-5</sup>	29±2.3	27±1.5
	with plasma	2.4 × 10 <sup>-1</sup>	71±1.7	69±1.7
AgNPs/PANi	without plasma	0.3456	90±2.3	90±1.8
	with plasma	0.6457	97±0.8	94±1.5

### 3.4. Antimicrobial activity

The antimicrobial properties of PANi and silver nanoparticles/PANi immobilized onto plasma-pretreated or untreated wool fibers are displayed in **Table 2**. The wool fibers were tested against *E. coli* and *S. aureus* applying plate agar counting. Blank wool displayed no antibacterial performance against the investigated bacterial pathogens; while AgNPs/PANi/wool fibers showed an improved antimicrobial performance compared to PANi/wool. Also, plasma-pretreated wool demonstrated higher antimicrobial performance compared to fibers without plasma-pretreatment. AgNPs have been reported as an efficient antibacterial agent against various bacterial, fungal and viral pathogenic organisms [49-52]. The actual mechanism of the toxic effects by AgNPs to pathogens is still partially documented [51, 52]. However, a number of mechanistic pathways were explored to explain the antibacterial behavior of silver nanoparticles. It was verified that raising the surface area of silver nanoparticles as a biologically active agent leads to improving their antimicrobial performance [53]. Hence, the bactericidal performance can be improved by providing additional amounts of silver nanoparticles in silver nanoparticles/PANi/wool. This was assigned to the penetration tendency of silver nanoparticles into DNA of bacteria and their discharging ability of Ag<sup>+</sup> throughout the bacteria cell-wall. Accordingly, Ag<sup>+</sup> interacts with phosphorous element of DNA molecules leading to functional inhibition of enzymes to result in bacterial death. Therefore, silver nanoparticles can be used to damaging plasmid and DNA of bacteria to result in improvement in antibacterial activity [54].

### 3.5. Coloration sensory and colorfastness measurements

Smart or interactive textiles can be classified as passive or active-based smart textile products. The passive-based smart fabrics are the earliest generations of smart textile products with the ability to afford additional characteristic in a passive form, such as the temperature insulator suit remains insulating irrespective of exterior temperature [55-67]. Other examples of passive smart textiles include antimicrobial, ultraviolet protective and antistatic fabrics. On the other side, the active smart textile products are the next generation including sensors and actuators. They are fabrics with the ability to automatically adapt their function

depending on changing environment, such as chromic textile products [68-76]. In this study, we described the development of active/passive hybrid wool fibers owing to their multifunctional performance, including thermochromism, vapochromism, acidochromism, metallochromism, electrical conductivity and antibacterial properties. The coloration parameters were recorded for each polyaniline derivative with and without plasma-activation as well as in presence and absence of AgNPs as depicted in **Table 3**.

**Table 3.** Coloration screening measurements for PANi/wool and AgNPs/PANi/wool.

Wool fabric		<i>K/S</i>	L*	a*	b*
Poly( <i>p</i> -nitroaniline)	Without plasma	18.29	63.15	5.22	45.16
	With plasma	21.21	50.98	8.32	34.85
AgNPs/PANi ( <i>p</i> -nitroaniline)	Without plasma	19.86	79.72	- 6.03	51.47
	With plasma	14.61	41.50	13.19	31.89
Poly( <i>o</i> -phenylenediamine)	Without plasma	19.36	40.32	12.72	30.45
	With plasma	23.42	37.70	14.77	34.81
AgNPs/PANi ( <i>o</i> -phenylenediamine)	Without plasma	17.24	44.46	13.31	41.34
	With plasma	17.24	48.50	14.78	44.84
Poly( <i>m</i> -anisidine)	Without plasma	10.78	39.35	7.98	15.68
	With plasma	11.06	35.27	8.77	16.78
AgNPs/PANi ( <i>m</i> -anisidine)	Without plasma	12.13	58.31	7.56	23.46
	With plasma	14.19	54.35	9.83	25.68

The treatment circumstances of wool played a considerable role in the behavior of the sensor wool fabric. The pristine wool showed an off-white shade with relatively high *K/S* (8.7), high L\* value (82.70), low negative a\* (- 0.71) and relatively high positive b\* (9.02). The *p*-nitroaniline afforded dark yellow-colored wool with considerably improved *K/S* and considerably decreased L\* for plasma-activated fibers and in the presence of AgNPs. The positive a\* and b\* noticeably increased for plasma-activated fibers and in the existence of silver nanoparticles to indicate dark yellow color. However, the positive a\* of plasma-inactivated AgNPs/PANi/wool exhibited a negative a\* value to designate a light pink color. Both of *o*-phenylenediamine and *m*-anisidine afforded yellow colored wool fabrics with considerably improved *K/S* and decreased L\* for plasma-treated fibers and in presence of silver nanoparticles presenting a dark yellow color. Both a\* and b\* possessed positive magnitudes and significantly increased for plasma-pretreated wool fibers and in presence of silver nanoparticles. Consequently, we elected *p*-nitroaniline as a key material in the sensor study owing to the considerable variations observed in presence of silver nanoparticles and upon plasma-pretreatment. Upon subjecting PANi/wool or AgNPs/PANi/wool to high temperature (~60-70°C) using hot air released from a heat gun, *K/S* values generally increased, while L\* values decreased to designate an improved color strength with an

immediate reversible color transformation (thermochromism) of darker yellow to bright light yellow.

**Table 4.** Color screening of wool fibers as sensor for high temperature (~60-70°C).

Wool fabric		K/S		L*		a*		b*	
		aq.	vapor	aq.	vapor	aq.	vapor	aq.	vapor
PANi	Without plasma	0.57	0.68	74.00	67.58	6.01	11.15	12.17	11.62
	With plasma	2.41	6.60	60.04	43.22	11.82	23.41	25.67	22.43
AgNPs/PANi	Without plasma	0.88	0.87	68.26	67.61	8.64	9.57	13.80	11.02
	With plasma	3.24	6.84	54.43	37.68	12.04	21.92	24.05	14.93

**Table 5.** Color screening of wool fibers as sensor for HCl under both aqueous and vapor conditions; PANi is derived from *p*-nitroaniline.

Wool fabric		K/S	L*	a*	b*
Poly( <i>p</i> -nitroaniline)	Without plasma	11.88	62.05	8.76	41.46
	With plasma	7.91	70.41	6.57	42.28
AgNPs/PANi ( <i>p</i> -nitroaniline)	Without plasma	11.82	62.05	8.77	41.42
	With plasma	12.84	51.00	9.21	30.31

**Table 6.** Color screening of wool fibers as sensor for metal ions (Fe(III) and Cu(II)); PANi is derived from *p*-nitroaniline.

Wool fabric		K/S		L*		a*		b*	
		Fe(III)	Cu(II)	Fe(III)	Cu(II)	Fe(III)	Cu(II)	Fe(III)	Cu(II)
PANi	Without plasma	1.41	1.29	69.32	68.5	9.95	6.35	20.39	14.36
	With plasma	4.03	3.87	56.48	53.18	13.17	9.11	31.32	23.31
AgNPs/PANi	Without plasma	1.55	1.23	68.77	66.99	14.06	8.70	27.11	15.57
	With plasma	5.59	6.86	48.62	41.88	15.75	11.87	32.10	20.12

**Table 7.** Fastness performance of Poly(*p*-nitroaniline)/wool and AgNPs/Poly(*p*-nitroaniline)/wool fibers with/without plasma pretreatment.

Wool fabric	Rubbing		Washing		Perspiration				Light
	Dry	Wet	Alt.*	St.*	Acidic		Alkaline		
					Alt.*	St.**	Alt.*	St.**	
PANi (plasma-pretreated)	3	3	3	2	2-3	2-3	3-4	3-4	3
PANi (plasma-activated)	3	3-4	3	3	3	2-3	3-4	3-4	4
PANi/AgNPs (plasma-inactivated)	3-4	3-4	4	3-4	3	3	3-4	3-4	4-5
PANi/AgNPs (plasma-activated)	4	4	4-5	4-5	4	4	4-5	4-5	6

\*Alt. is alteration; \*\*St. is staining.

No significant changes were detected for either  $a^*$  or  $b^*$  values (Table 4). However, the plasma-inactivated AgNPs/PANi/wool showed a significant alteration from negative to positive magnitudes associated with an instantaneous reversible color transformation of light pink to bright light yellow. Analogous behaviors were observed for wool sensing both HCl aqueous (halochromism) and vapor (vapochromism) phases (Table 5), as well as metal ions (metallochromism) including Fe(III) and Cu(II) (Table 6) showing an instantaneous and reversible colorimetric shifting from dark yellowish to brighter light yellowish or from light pink to bright light yellow for plasma-activated and plasma-inactivated AgNPs/PANi/wool samples, respectively. The sensory effects generated by PANi/wool and AgNPs/PANi/wool fabrics depended mainly on changes of the physical and chemical characteristics of the samples during the sensing course.

The colorfastness performance of the treated wool substrates showed satisfactory results to maintain their color against rubbing, perspiration, light and washing. Considerable enhancements in the colorfastness were monitored upon moving from PANi/wool to AgNPs/PANi/wool fibers. Moreover, the plasma-pretreated substrates showed better colorfastness than that of the plasma-inactivated substrates. The best fastness properties were monitored between good and very good for plasma-activated Ag NPs/PANi/wool (Table 7). This can be assigned to strong chemically bind of AgNPs/PANi to plasma-activated fibers to confirm product robustness. The strong Ag-O bond was stabilized by AgNPs/PANi within wool fibrous matrix. This uncovered the ability of this proposed technique to achieve satisfactory coloration process toward multifunctional textiles of satisfactory colorfastness properties without applying any additional chemicals.

#### 4. Conclusions

Facile strategy was introduced toward the development of multiple functional wool imparted antimicrobial activity, electroactivity, thermochromism, acidochromism, metallochromism and vapochromism employing AgNPs/PANi coating. The dispersion of AgNO<sub>3</sub> and *in-situ* polymerization of arylamine derivatives can efficiently introduce thin layer of silver nanoparticles/PANi onto plasma-treated wool. The morphologies and elemental content of the coated substrates were studied by several methods, including SEM, EDX and FTIR. SEM images showed nano(micro)-sized particles incorporated onto the surface of the coated substrates, while EDX proved the existence of metallic silver in the chemical composition of the treated wool fibers. AgNPs increased the electroactivity of AgNPs/PANi/wool by improving the consistent dispersion of silver nanoparticles/PANi onto the fabric. The electroconductivity of AgNPs/PANi/wool samples was as high as 0.6457 S/cm, which increased about  $\sim 5.4 \times 10^7$  times compared to the value of blank wool at  $1.2 \times 10^{-8}$  S cm<sup>-1</sup>. The antimicrobial activity of AgNPs/PANi/wool against *E. coli* and *S. aureus* was considerably increased compared to PANi/wool, whereas the blank wool did not display any antibacterial properties. The colorfastness demonstrated satisfactory performance of PANi and AgNPs/PANi composites incorporated onto wool fibers. AgNPs/PANi/wool fibers were able to illustrate color shifts upon exposing to heating, strong acid and metallic ions demonstrating metallochromic, acidochromic, vapochromic

and thermochromic sensory effects. This simple approach is characterized with fast response and operation under ambient conditions, which will open the door for chromic wearable materials for protective healthcare applications.

#### Acknowledgements

Technical and financial support from National Research Centre, Cairo, Egypt (Grant # 12010206); is gratefully acknowledged.

#### Declaration of Competing Interest

The authors declare that there is no conflict of interest.

#### References

- [1] T.A. Khattab, M.M.G. Fouda, A.A. Allam, S.I. Othman, M. Bin-Jumah, H.M. Al-Harbi, M. Rehan, Selective Colorimetric Detection of Fe (III) Using Metallochromic Tannin-Impregnated Silica Strips, *ChemistrySelect* 3(43) (2018) 12065-12071.
- [2] S. Yasin, D. Sun, Propelling textile waste to ascend the ladder of sustainability: EOL study on probing environmental parity in technical textiles, *J. Clean. Prod.* 233 (2019) 1451-1464.
- [3] T.A. Khattab, S. Dacrory, H. Abou-Yousef, S. Kamel, Smart microfibrillated cellulose as swab sponge-like aerogel for real-time colorimetric naked-eye sweat monitoring, *Talanta* 205 (2019) 120166.
- [4] M. Sun, J. Lv, H. Xu, L. Zhang, Y. Zhong, Z. Chen, X. Sui, B. Wang, X. Feng, Z. Mao, Smart cotton fabric screen-printed with viologen polymer: photochromic, thermochromic and ammonia sensing, *Cellulose* 27(5) (2020) 2939-2952.
- [5] T.A. Khattab, M.M.G. Fouda, M.S. Abdelrahman, S.I. Othman, M. Bin-Jumah, M.A. Alqaraawi, H. Al Fassam, A.A. Allam, Co-encapsulation of enzyme and tricyanofuran hydrazone into alginate microcapsules incorporated onto cotton fabric as a biosensor for colorimetric recognition of urea, *React. Funct. Polym.* 142 (2019) 199-206.
- [6] F. Fan, W. Zhang, C. Wang, Covalent bonding and photochromic properties of double-shell polyurethane-chitosan microcapsules crosslinked onto cotton fabric, *Cellulose* 22(2) (2015) 1427-1438.
- [7] W. Weng, P. Chen, S. He, X. Sun, H. Peng, Smart electronic textiles, *Angew. Chem. Int. Ed.* 55(21) (2016) 6140-6169.
- [8] A. Abdollahi, H. Roghani-Mamaqani, B. Razavi, Stimuli-chromism of photoswitches in smart polymers: Recent advances and applications as chemosensors, *Prog. Polym. Sci.* 98 (2019) 101149.
- [9] T.A. Khattab, S. Mowafi, H. El-Sayed, Development of mechanically durable hydrophobic lanolin/silicone rubber coating on viscose fibers, *Cellulose* 26 (17) (2019) 9361-9371.
- [10] T.A. Khattab, From chromic switchable hydrazones to smart materials, *Mater. Chem. Phys.* 254 (2020) 123456.
- [11] E.T. Alonso, D.P. Rodrigues, M. Khetani, D.-W. Shin, A. De Sanctis, H. Joulie, I. de Schrijver, A. Baldycheva, H. Alves, A.I. Neves, S. Russo, M.F. Cracium, Graphene electronic fibres with touch-sensing and light-emitting functionalities for smart textiles." *npj Flex. Electron.* 2(1) (2018) 1-6.
- [12] L. Veeramuthu, W.-L. Li, F.-C. Liang, C.-J. Cho, C.-C. Kuo, W.-C. Chen, J.-H. Lin, W.-Y. Lee, C.-T.

- Wang, W.-Y. Lin, S.-P. Rwei, Smart garment energy generators fabricated using stretchable electrospun nanofibers, *React. Funct. Polym.* 142 (2019) 96-103.
- [13] D.J. Roach, C. Yuan, X. Kuang, V.C.-F. Li, P. Blake, M.L. Romero, I. Hammel, K. Yu, H.J. Qi, Long liquid crystal elastomer fibers with large reversible actuation strains for smart textiles and artificial muscles, *ACS Appl. Mater. Interfaces* 11(21) (2019) 19514-19521.
- [14] T.A. Khattab, S. Dacrory, H. Abou-Yousef, S. Kamel, Development of microporous cellulose-based smart xerogel reversible sensor via freeze drying for naked-eye detection of ammonia gas, *Carbohydr. polym.* 210 (2019) 196-203.
- [15] S. Karppinen, V. Kallunki, K. Komulainen, Interdisciplinary craft designing and invention pedagogy in teacher education: student teachers creating smart textiles, *Int. J. Technol. Des. Ed.* 29(1) (2019) 57-74.
- [16] M.G. Honarvar, M. Latifi, Overview of wearable electronics and smart textiles, *J. Text. I.* 108 (4) (2017) 631-652.
- [17] M.S. Abdelrahman, T.A. Khattab, Development of One-Step Water-Repellent and Flame-Retardant Finishes for Cotton, *ChemistrySelect* 4(13) (2019) 3811-3816.
- [18] M. Akhtar, H.A. Weakliem, R.M. Paiste, K. Gaughan, Polyaniline thin film electrochromic devices, *Synthetic metals* 26(3) (1988) 203-208.
- [19] T.A. Khattab, N.F. Kassem, A.M. Adel, S. Kamel, Optical Recognition of Ammonia and Amine Vapor Using "Turn-on" Fluorescent Chitosan Nanoparticles Imprinted on Cellulose Strips, *J. Fluoresc.* 29 (3) (2019) 693-702.
- [20] J. Lai, Y. Yi, P. Zhu, J. Shen, K. Wu, L. Zhang, J. Liu, Polyaniline-based glucose biosensor: A review, *J. Electroanal. Chem.* 782 (2016) 138-153.
- [21] M. Yanilmaz, A.S. Sarac, A review: effect of conductive polymers on the conductivities of electrospun mats, *Text. Res. J.* 84(12) (2014) 1325-1342.
- [22] Y. Jiang, Z. Liu, G. Zeng, Y. Liu, B. Shao, Z. Li, Y. Liu, W. Zhang, Q. He, Polyaniline-based adsorbents for removal of hexavalent chromium from aqueous solution: a mini review, *Environ. Sci. Pollut. Res.* 25(7) (2018) 6158-6174.
- [23] Y. Wang, A. Liu, Y. Han, T. Li, Sensors based on conductive polymers and their composites: a review, *Polym. Int.* 69(1) (2020) 7-17.
- [24] S.K. Kandasamy, K. Kandasamy, Recent advances in electrochemical performances of graphene composite (graphene-polyaniline/polypyrrole/activated carbon/carbon nanotube) electrode materials for supercapacitor: A review, *J Inorg. Organomet. Polym. Mater.* 28(3) (2018) 559-584.
- [25] E.N. Zare, A. Motahari, M. Sillanpää, Nanoadsorbents based on conducting polymer nanocomposites with main focus on polyaniline and its derivatives for removal of heavy metal ions/dyes: a review, *Environ. Res.* 162 (2018) 173-195.
- [26] Z. Huang, L. Li, Y. Wang, C. Zhang, T. Liu, Polyaniline/graphene nanocomposites towards high-performance supercapacitors: a review, *Compos. Commun.* 8 (2018) 83-91.
- [27] W.J.E. Beek, M.M. Wienk, R.A.J. Janssen, Efficient hybrid solar cells from zinc oxide nanoparticles and a conjugated polymer, *Adv. Mater.* 16(12) (2004) 1009-1013.
- [28] I. Choi, D. Lee, Radar absorbing composite structures dispersed with nano-conductive particles, *Compos. Struct.* 122 (2015) 23-30.
- [29] A. Afzali, V. Mottaghitalab, S.S. Afghahi, M. Jafarian, The coating of composite nanoparticles of BaFe<sub>2</sub>O<sub>7</sub>/multi-walled carbon nanotubes using silicon matrix on nonwoven substrate for radar absorption in X and Ku bands, *J. Ind. Text.* 47(8) (2018) 1867-1886.
- [30] A.M. El-Nahrawy, A.B. Abou Hammad, T.A. Khattab, A. Haroun, S. Kamel, Development of electrically conductive nanocomposites from cellulose nanowhiskers, polypyrrole and silver nanoparticles assisted with Nickel (III) oxide nanoparticles, *React. Funct. Polym.* 149 (2020) 104533.
- [31] S. Prabhu, E.K. Poulouse, Silver nanoparticles: mechanism of antimicrobial action, synthesis, medical applications, and toxicity effects, *Int. Nano Lett.* 2(1) (2012) 32.
- [32] Y.-W. Nam, J.-H. Choi, W.-J. Lee, C.-G. Kim, Thin and lightweight radar-absorbing structure containing glass fabric coated with silver by sputtering, *Compos. Struct.* 160 (2017) 1171-1177.
- [33] V. Babaahmadi, M. Montazer, W. Gao, Low temperature welding of graphene on PET with silver nanoparticles producing higher durable electro-conductive fabric, *Carbon* 118 (2017) 443-451.
- [34] I. Fratoddi, I. Venditti, C. Cametti, M.V. Russo, Chemiresistive polyaniline-based gas sensors: A mini review, *Sens. Actuators B Chem.* 220 (2015) 534-548.
- [35] T.H. Qazi, R. Rai, A.R. Boccaccini, Tissue engineering of electrically responsive tissues using polyaniline based polymers: a review, *Biomaterials* 35(33) (2014) 9068-9086.
- [36] A.A. Khan, M. Khalid, U. Baig, Synthesis and characterization of polyaniline-titanium (IV) phosphate cation exchange composite: methanol sensor and isothermal stability in terms of DC electrical conductivity, *React. Funct. Polym.* 70(10) (2010) 849-855.
- [37] H. Zhao, L. Hou, S. Bi, Y. Lu, Enhanced X-band electromagnetic-interference shielding performance of layer-structured fabric-supported polyaniline/cobalt-nickel coatings, *ACS Appl. Mater. Interfaces* 9(38) (2017) 33059-33070.
- [38] X. Cheng, V. Kumar, T. Yokozeki, T. Goto, T. Takahashi, J. Koyanagi, L. Wu, R. Wang, Highly conductive graphene oxide/polyaniline hybrid polymer nanocomposites with simultaneously improved mechanical properties, *Compos. Part A Appl. Sci. Manuf.* 82 (2016) 100-107.
- [39] J.G. Alonso, C. Dalmolin, J. Nahorny, A.A.C. Recco, L.C. Fontana, D. Becker, Active screen plasma system applied to polymer surface modification: poly (lactic acid) surface activation before polyaniline graft polymerization in aqueous medium, *J. Polym. Eng.* 38 (8) (2018) 795-802.
- [40] J. Qian, C. Wen, J. Xia, Development of highly efficient chemosensors for Cu<sup>2+</sup> and N<sub>2</sub>H<sub>4</sub> detection based on 2D polyaniline derivatives by template-free

- chemical polymerization method, *J. Hazard. Mater.* 389 (2020) 121902.
- [41] R. Wang, Q. Wu, X. Zhang, Z. Yang, L. Gao, J. Ni, O.K.C. Tsui, Flexible supercapacitors based on a polyaniline nanowire-infilled 10 nm-diameter carbon nanotube porous membrane by in situ electrochemical polymerization, *J. Mater. Chem. A* 4(32) (2016) 12602-12608.
- [42] S. Park, H.-S. Kil, D. Choi, S.-K. Song, S. Lee, Rapid stabilization of polyacrylonitrile fibers achieved by plasma-assisted thermal treatment on electron-beam irradiated fibers, *J. Ind. Eng. Chem.* 69 (2019) 449-454.
- [43] M. Nazari, S. Agbolaghi, H. Gheybi, S. Abbaspoor, F. Abbasi, A focus on the features of polyaniline nanofibres prepared via developing the single crystals of their block copolymers with poly (ethylene glycol), *Bull. Mater. Sci.* 41(1) (2018) 29.
- [44] H. Ahmed, T.A. Khattab, H.M. Mashaly, A.A. El-Halwagy, M. Rehan, Plasma activation toward multi-stimuli responsive cotton fabric via in situ development of polyaniline derivatives and silver nanoparticles, *Cellulose* 27(5) (2020) 2913-2926.
- [45] K.V. Rani, B. Sarma, A. Sarma, Plasma treatment on cotton fabrics to enhance the adhesion of Reduced Graphene Oxide for electro-conductive properties, *Diam. Relat. Mater.* 84 (2018) 77-85.
- [46] T.A. Khattab, M.H. Elnagdi, K.M. Haggaga, A.A. Abdelrahmana, S.A. Aly, Green synthesis, printing performance, and antibacterial activity of disperse dyes incorporating arylazopyrazolopyrimidines, *AATCC J. Res.* 4(4) (2017) 1-8.
- [47] T.A. Khattab, Novel solvatochromic and halochromic sulfahydrazone molecular switch, *J. Mol. Struct.* 1169 (2018) 96-102.
- [48] K. Jyoti, M. Baunthiyal, A. Singh, Characterization of silver nanoparticles synthesized using *Urtica dioica* Linn. leaves and their synergistic effects with antibiotics, *J. Radiat. Res. Appl. Sci.* 9(3) (2016) 217-227.
- [49] S.S. Rao, K. Saptami, J. Venkatesan, P.D. Rekha, Microwave-assisted rapid synthesis of silver nanoparticles using fucoidan: Characterization with assessment of biocompatibility and antimicrobial activity, *Int. J. Biol. Macromol.* 163 (2020) 745-755.
- [50] M.E. El-Naggar, T.A. Khattab, M.S. Abdelrahman, A. Aldalbahi, M.R. Hatshan, Development of antimicrobial, UV blocked and photocatalytic self-cleanable cotton fibers decorated with silver nanoparticles using silver carbamate and plasma activation, *Cellulose* 28 (2021) 1105-1121.
- [51] D. Garibo, H.A. Borbón-Nuñez, J.N.D. de León, E.G. Mendoza, I. Estrada, Y. Toledano-Magaña, H. Tiznado, M. Ovalle-Marroquin, A.G. Soto-Ramos, A. Blanco, J.A. Rodríguez, Green synthesis of silver nanoparticles using *Lysiloma acapulcensis* exhibit high-antimicrobial activity, *Sci. Rep.* 10(1) (2020) 1-11.
- [52] M. Rehan, A.A. Nada, T.A. Khattab, N.A.M. Abdelwahed, A.A. Abou El-Kheir, Development of multifunctional polyacrylonitrile/silver nanocomposite films: Antimicrobial activity, catalytic activity, electrical conductivity, UV protection and SERS-active sensor, *J. Mater. Res. Technol.* 9(4) (2020) 9380-9394.
- [53] M. Rai, A. Yadav, A. Gade, Silver nanoparticles as a new generation of antimicrobials, *Biotechnol. Adv.* 27(1) (2009) 76-83.
- [54] M.A. Radzig, V.A. Nadochenko, O.A. Koksharova, J. Kiwi, V.A. Lipasova, I.A. Khmel, Antibacterial effects of silver nanoparticles on gram-negative bacteria: influence on the growth and biofilms formation, mechanisms of action, *Colloids Surf. B* 102 (2013) 300-306.
- [55] T.A. Khattab, H.E. Gaffer, S. Abdelmoez Aly, T.M. Klapötke, Synthesis, solvatochromism, antibacterial activity and dyeing performance of tricyanofuran-hydrazone analogues, *ChemistrySelect* 1(21) (2016) 6805-6809.
- [56] H. Abou-Yousef, T.A. Khattab, Y.A. Youssef, N. Al-Balakocy, S. Kamel, Novel cellulose-based halochromic test strips for naked-eye detection of alkaline vapors and analytes, *Talanta* 170 (2017) 137-145.
- [57] T.A. Khattab, K.M. Haggag, M.H. Elnagdi, A.A. Abdelrahman, S. Abdelmoez Aly, Microwave-assisted synthesis of arylazoaminopyrazoles as disperse dyes for textile printing, *Z. Anorg. Allg. Chem.* 642(13) (2016) 766-772.
- [58] A.F. Little, R.M. Christie, Textile applications of photochromic dyes. Part 1: establishment of a methodology for evaluation of photochromic textiles using traditional colour measurement instrumentation, *Color. Technol.* 126(3) (2010) 157-163.
- [59] M.S. Abdelrahman, H. Ali, Boron Difluoride Complex Dyes: Synthesis and Photophysical Properties, *J. Text. Color. Polym. Sci.* 17(1) (2020) 43-55.
- [60] S. Abdelmoez, M. Abdelrahman, T. Khattab, Synthesis, Solvatochromic Properties and pH Sensory of Novel Symmetrical Bis (Tricyanofuran) hydrazone Chromophore, *Egypt. J. Chem.* 62(7) (2019) 1197-1206.
- [61] M.S. Abdelrahman, T.A. Khattab, S. Kamel, Development of a novel colorimetric thermometer based on poly (N-vinylcaprolactam) with push- $\pi$ -pull tricyanofuran hydrazone anion dye, *New J. Chem.* 45(12) (2021) 5382-5390.
- [62] H. Mohamed, S. Taher, A. El-Halwagy, A. Abdelrahman, A. Garamoon, Surface Characteristics and Printing Properties of Cotton Fabric Treated with Dielectric Barrier Discharge, *J. Text. Color. Polym. Sci.* 16(2) (2019) 165-185.
- [63] M.S. Abdelrahman, T.A. Khattab, S. Kamel, Hydrazone-Based Supramolecular Organogel for Selective Chromogenic Detection of Organophosphorus Nerve Agent Mimic, *ChemistrySelect* 6(9) (2021) 2002-2009.
- [64] T.A. Khattab, S. Abdelmoez Aly, T.M. Klapötke, Naked-eye facile colorimetric detection of alkylphenols using Fe (III)-impregnated silica-based strips, *Chem. Pap.* 72(6) (2018) 1553-1559.
- [65] M.S. Abdelrahman, M.M.G. Fouda, J.S. Ajarem, S.N. Maooda, A.A. Allam, T.A. Khattab, Development of colorimetric cotton swab using molecular switching hydrazone probe in calcium alginate, *J. Mol. Struct.* 1216 (2020) 128301.
- [66] F. Fan, Y. Wu, Photochromic properties of color-matching, double-shelled microcapsules covalently bonded onto cotton fabric and applications

- to outdoor clothing, *J. Appl. Polym. Sci.* 134(15) (2017) 44698.
- [67] M.M. Abdelhameed, Y.A. Attia, M.S. Abdelrahman, T.A. Khattab, Photochromic and fluorescent ink using photoluminescent strontium aluminate pigment and screen printing towards anticounterfeiting documents, *Luminescence* 36(4) (2021) 865-874.
- [68] M. S. Abdelrahman, H. N. Sahar, H. Mashaly, S. Mahmoud, D. Maamoun, Synthesis and Characterization of Biodegradable Synthetic Thickener from Anionic Triglyceride Poly(lactic Acid), *Appl. Ecol. Environ. Sci* 6 (2018) 35-47.
- [69] T.A. Khattab, M.E. El-Naggar, M.S. Abdelrahman, A. Aldalbahi, M.R. Hatshan, Facile development of photochromic cellulose acetate transparent nanocomposite film immobilized with lanthanide-doped pigment: ultraviolet blocking, superhydrophobic, and antimicrobial activity, *Luminescence* 36(2) (2021) 543-555.
- [70] T.A. Khattab, M. Rehan, Synthesis and characterization of bis-azo 1, 2, 4, 5-tetrazine dyestuff, *J. Text. Color. Polym. Sci.* 15(1) (2018) 33-36.
- [71] E. Abdel-latif, A. Mansour, E. Abdel-Galil, Solvent Effects on the UV-visible Absorption Spectra of some New Thienylazo-thiazole and Thienylazo-thiophene Dyes, *J. Text. Color. Polym. Sci.* 15(1) (2018) 1-13.
- [72] T.A. Khattab, E. Tolba, H. Gaffer, S. Kamel, Development of electrospun nanofibrous-walled tubes for potential production of photoluminescent endoscopes, *Ind. Eng. Chem. Res.* 60(28) (2021) 10044-10055.
- [73] T.A. Khattab, M.E. El-Naggar, M.S. Abdelrahman, A. Aldalbahi, M.R. Hatshan, Simple Development of Novel Reversible Colorimetric Thermometer Using Urea Organogel Embedded with Thermochromic Hydrazone Chromophore, *Chemosensors* 8(4) (2020) 132.
- [74] H. Mohamed, A.A. EL-Hahwagy, Plasma-based Nanotechnology for Textile Coating, *J. Text. Color. Polym. Sci.* 18(1) (2021) 11-31.
- [75] S. Kamel, T.A. Khattab, Recent advances in cellulose supported metal nanoparticles as green and sustainable catalysis for organic synthesis, *Cellulose* 28 (2021) 4545-4574.
- [76] M. Abdelrahman, S. Wahab, H. Mashaly, D. Maamoun, T.A. Khattab, Review in Textile Printing Technology, *Egypt. J. Chem.* 63(9) (2020) 2-3.
- [77] A.L. Mohamed, A.G. Hassabo, Review of silicon-based materials for cellulosic fabrics with functional applications, *J. Text. Color. Polym. Sci.* 16(2) (2019) 139-157.
- [78] T.A. Khattab, K.M. Haggag, Synthesis and spectral properties of symmetrical and asymmetrical 3-cyano-1, 5-diarylformazan dyestuffs for dyeing polyester fabrics, *Egypt. J. Chem.* 60 (2017) 33-40.
- [79] T.A. Khattab, Synthesis and Self-assembly of Novel s-Tetrazine-based Gelator, *Helv. Chim. Acta* 101(4) (2018) e1800009.
- [80] H. Gaffer, T. Khattab, Synthesis and characterization of some azo-heterocycles incorporating pyrazolopyridine moiety as disperse dyes, *Egypt. J. Chem.* 60 (2017) 41-47.
- [81] M.E. El-Naggar, M.H. El-Newehy, A. Aldalbahi, W.M. Salem, T.A. Khattab, Immobilization of anthocyanin extract from red-cabbage into electrospun poly(vinyl alcohol) nanofibers for colorimetric selective detection of ferric ions, *J. Environ. Chem. Eng.* 9(2) (2021) 105072.
- [82] M.S. Abdelrahman, T.A. Khattab, A. Aldalbahi, M.R. Hatshan, M.E. El-Naggar, Facile development of microporous cellulose acetate xerogel immobilized with hydrazone probe for real time vapochromic detection of toxic ammonia, *J. Environ. Chem. Eng.* 8(6) (2020) 104573.
- [83] N.A. Alhakamy, A.O. Noor, K.M. Hosny, J.J. Nasr, M.M.G. Fouda, T.A. Khattab, H.E. Gaffer, Synthesis of new cyanopyridine scaffolds and their biological activities, *Curr. Org. Synth.* 17(7) (2020) 567-575.
- [84] M.E. El-Naggar, O.A. Abu Ali, D.I. Saleh, M.A. Abu-Saied, T.A. Khattab, Preparation of green and sustainable colorimetric cotton assay using natural anthocyanins for sweat sensing, *Int. J. Biol. Macromol.* 190 (2021) 894-903.
- [85] M. Yousef, H. Othman, A.G. Hassabo, A Recent Study for Printing Polyester Fabric with Different Techniques, *J. Text. Color. Polym. Sci.* 18(2) (2021) 247-252.
- [86] T.A. Khattab, S. Kamel, A Concise Review on Synthesis and Applications of Helicenes, *Egypt. J. Chem.* 64(2) (2021) 4-7.
- [87] T.A. Khattab, M.S. Abdelrahman, H.B. Ahmed, H.E. Emam, Molecularly Imprinted Cellulose Sensor Strips for Selective Determination of Phenols in Aqueous Environment, *Fibers Polym.* 21(10) (2020) 2195-2203.